The solvent sensitivity ($B = \nu_{max}/E^*_{MLCT}$) of the MLCT transition energy for the $[M(CO)_4]$dpp and $[M(CO)_4]_2$dpp complexes decreases slightly in the order M = Mo > W > Cr. The B value for $[Mo(CO)_4]$dpp of 3058 is an intermediate value between the extremes for $[Mo(CO)_4]$bpm (B = 4100, bpm = 4,4′-bipyrimidine) and $[Mo(CO)_4]$abpy (B = 560, abpy = azo-2,2′-bis(pyridine)).[18,20] On the basis of comparative B values with other $[Mo(CO)_4]$L complexes, this result suggests ddp is less effective at π back-donation than L = bpy, bpm, bpym, 2,2′-bipyrazine (bpz), or 3,3′-bipyridazine (bpdz).[18-20] The B value for $[Mo(CO)_4]_2$dpp of 3256 also falls between extremes ($[Mo(CO)_4]_2$bpym, B = 4110; $[Mo(CO)_4]_2$abpy, B = 1460) and most closely approximates the value of 3110 reported for the isomeric 2,5-bis(2-pyridyl)pyrazine (dppz) ligand complex $[Mo(CO)_4]_2$dppz.[18-20] These results are consistent with previous solvatochromic studies which suggested that metal centers bound to stronger bases such as pyrimidines and pyrazines (greater σ donation) are more polarizable in the ground state than metal centers bound to weaker bases. The B values of the bimetallic dpp complexes (except Cr–Cr) are larger than those of the respective monometallic dpp complexes, consistent with two polarizable metal centers.[18] The B value decreases for heterobimetallic complexes in the order Mo–W > Mo–Cr > W–Cr as could be predicted from B values of the monometallic complexes.

The energy of the MLCT absorption in a given solvent decreased in the order M = Mo > W > Cr for $[M(CO)_4]$dpp complexes and Mo–Mo > Mo–W > Mo–Cr > W–W > W–Cr ≥ Cr–Cr for $[M(CO)_4]$dpp$[M'(CO)_4]$ complexes. The decreasing energy trend for the monometallic series is consistent with that for other complexes of group 6 metal carbonyls.[20,21]

^{13}C NMR spectra for dpp and bimetallic dpp-bridged complexes were recorded in deuteriated dichloromethane (Table IV). The assignment of dpp signals is based on those for bpy and bpym.[16,22] Assignment of signals for homobimetallic complexes is based on dpp, and heterobimetallic signals are interpreted from the relative amount of shift from each metal in the homobimetallic complex. All ^{13}C signals in the bimetallic complexes shifted downfield (vs dpp), indicating stronger σ-donating effects predominate vs π-back-bonding contributions. The relative order of downfield shift for a carbon in homobimetallic complexes (M = Cr > W > Mo) parallels previous results for bpym complexes.[16,22]

Acknowledgment. We gratefully acknowledge the generous financial support of this work from the Research Corp.

Registry No. $[Cr(CO)_4]_2$dpp, 111468-79-2; $[W(CO)_4]_2$dpp, 111468-80-5; $[Mo(CO)_4]$dpp$[W(CO)_4]$, 111468-81-6; $[Mo(CO)_4]$dpp$[Cr(CO)_4]$, 111468-82-7; $[W(CO)_4]$dpp$[Cr(CO)_4]$, 111468-83-8; $[Cr(CO)_4]$dpp, 111468-84-9; $[Mo(CO)_4]_2$dpp, 105969-43-5; $[Mo(CO)_4]$dpp, 105969-42-4; $[W(CO)_4]$dpp, 111489-99-7; $W(CO)_6$, 14040-11-0; $Cr(CO)_6$, 13007-92-6; $Mo(CO)_6$, 13939-06-5.

Contribution from the Department of Chemistry, Faculty of Science and Engineering, Saga University, Honjo-machi, Saga, 840 Japan, and Laboratory of Analytical Chemistry, Faculty of Science, Nagoya University, Chikusa-ku, Nagoya, 464 Japan

Importance of Hydrophobic Interaction in Metalloporphyrin Formation

Masaaki Tabata[1a] and Motoharu Tanaka*[1b]

Received July 30, 1987

Kinetic studies of metalloporphyrin formation may be helpful to understand the in vivo metal incorporation processes leading to the heme and chlorophylls.[2,3] The last step of the heme biosynthesis is the incorporation of iron(II) into protoporphyrin IX. The reaction does not occur readily and requires the enzyme of ferrochelatase.[4-6] Large metal ions such as mercury(II), cadmium(II), or lead(II) have been found to catalyze the metalloporphyrin formation.[7,8]

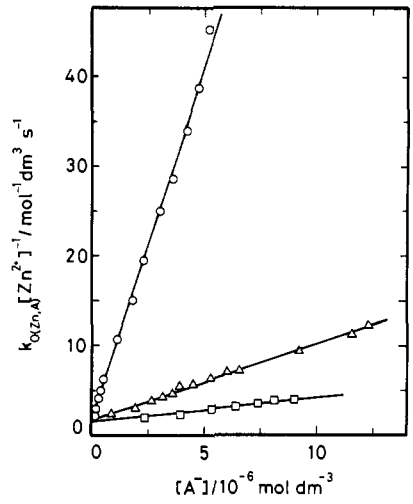

Figure 1. Plots of $k_{0(Zn,A)}[Zn^{2+}]^{-1}$/mol^{-1} dm^3 s^{-1} vs [A$^-$]/10^{-6} mol dm^{-3} for L-tryptophan (○), L-phenylalanine (△), and glycine (□), where A$^-$ denotes the anionic form of amino acid.

The present paper describes a catalytic effect of amino acids on the rate of metalloporphyrin formation. The reaction of zinc(II) with 5,10,15,20-tetrakis(4-sulfonatophenyl)porphine (H_2TPPS_4; charges on porphyrin and metalloporphyrin are omitted throughout) was found to be accelerated by amino acids (HA: glycine (Gly), L-α-alanine (Ala), L-valine (Val), L-phenylalanine (Phe), L-tyrosine (Tyr), and L-tryptophan (Trp), where HA denotes neutral form of amino acid). The catalytic effect of amino acids is discussed in terms of hydrophobic interaction of the amino acid side chain with porphyrin. The enhanced rate constant in the presence of amino acids is correlated with the hydrophobicity scale of amino acid residue.[9]

Kinetic studies were carried out in the pH range 6.0–7.0 (*N*,*N*′-bis(2-sulfonatoethyl)piperazine (PIPES) buffer, 5.0 × 10^{-3} mol dm^{-3}), at various concentrations of amino acid (1 × 10^{-5} to 4 × 10^{-2} mol dm^{-3}) and of zinc(II) (1 × 10^{-4} to 2 × 10^{-3} mol dm^{-3}) at 25 °C and I = 0.1 mol dm^{-3} ($NaNO_3$). The reaction was started by mixing a solution containing zinc(II) and amino acid with an H_2TPPS_4 solution (1.05 × 10^{-6} mol dm^{-3}). The change in absorbance at 421 nm (Soret band of $Zn^{II}(TPSS_4)$) was monitored as a function of time. The conditional formation rate constant of $Zn^{II}(TPPS_4)$, k_0, involving concentrations of hydrogen, zinc(II), and amino acid was determined from the first-order

* To whom correspondence should be addressed.

(1) (a) Saga University. (b) Nagoya University.
(2) Tanaka, M. *Pure Appl. Chem.* **1983**, *55*, 151–158, and references therein.
(3) Lavallee, D. K. *Coord. Chem. Rev.* **1985**, *61*, 55–96, and references therein.
(4) Jones, M. S.; Jones, O. T. G. *Biochem. J.* **1970**, *119*, 453–462.
(5) Dailey, H. A., Jr.; Lascelles, J. *Arch. Biochem. Biophys.* **1974**, *160*, 523–529.
(6) Camadro, J. M.; Labbe, P. *Biochim. Biophys. Acta* **1982**, *707*, 280–288.
(7) (a) Tabata, M.; Tanaka, M. *Inorg. Chim. Acta Lett.* **1980**, *40*, X71. (b) Tabata, M.; Tanaka, M. *Anal. Lett.* **1980**, *13*(A6), 427–438. (c) Tabata, M.; Tanaka, M. *Mikrochim. Acta* **1982**, 149–158. (d) Tabata, M.; Tanaka, M. *J. Chem. Soc., Dalton Trans.* **1983**, 1955–1959. (e) Tabata, M. *Analyst (London)* **1987**, *112*, 141–144.
(8) Haye, S. E.; Hambright, P. *Inorg. Chem.* **1984**, *23*, 4777–4779.
(9) Nozaki, Y.; Tanford, C. *J. Biol. Chem.* **1971**, 246, 2211–2217. The hydrophobicity scale was experimentally determined by free energy of transfer of amino acids from water to organic solvent, and the value was recently used to analyze amino acid residues in globular proteins: Rose, G. D.; Geselowitz A. R.; Lesser, G. J.; Lee, R. H.; Zehfus, M. H. *Science (Washington, D.C.)* **1985**, *229*, 834–838.

0020-1669/88/1327-0203$01.50/0

Table I. Formation Rate Constant of $Zn^{II}(TPPS_4)$ in the Presence of Amino Acids (HA) at I = 0.1 mol dm^{-3} and 25 °C

HA	k_{ZnA}/mol^{-1} dm^3 s^{-1}	Δg_t^a/kJ mol^{-1}
H_2O	1.59 ± 0.09	
Gly	3.60 ± 0.10	0.0
Ala	12.0 ± 0.5	2.1
Val	19.9 ± 0.9	6.3
Phe	43.0 ± 0.8	10.5
Tyr	52.7 ± 0.8	9.6
Trp	82.2 ± 6.9	14.2

[a] hydrophobicity scale of amino acid side-chain: Nozaki, Y.; Tanford, C. *J. Biol. Chem.* **1971**, *246*, 2211–2217.

kinetic plot. The kinetics of $Zn(TPPS_4)$ formation in the presence of amino acid is of the form

$$k_{0(Zn,A)} = k_1[Zn^{2+}] + k_2[ZnA^+] + k_3[ZnA_2] \quad (1)$$

$$= k_1[Zn^{2+}] + k_2\beta_1[Zn^{2+}][A^-] + k_3\beta_2[Zn^{2+}][A^-]^2 \quad (2)$$

where values β_1 and β_2, for the overall formation constants of ZnA^+ and ZnA_2, were taken from the literature.[10] Concentrations of Zn^{2+} and A^- were calculated by eq 3 and 4, where C_{Zn} and C_{HA}

$$C_{Zn} = [Zn^{2+}] + [ZnA^+] + [ZnA_2] = [Zn^{2+}](1 + \beta_1[A^-] + \beta_2[A^-]^2) \quad (3)$$

$$C_{HA} = [HA] + [ZnA^+] + 2[ZnA_2] = [A^-]([H^+]K_a^{-1} + \beta_1[Zn^{2+}] + 2\beta_2[Zn^{2+}][A^-]^2) \quad (4)$$

are the total concentrations of zinc and amino acid, respectively, and K_a is the proton dissociation constant of the amino acid. Formation of ZnA_2 is a few percent at most under the present experimental conditions; for example, the distributions of Zn^{2+}, ZnA^+, and ZnA_2 for glycine are 65%, 32%, and 3% at $C_{HA} = 2.79 \times 10^{-2}$ mol dm^{-3} and pH 6.37. Zinc(II) hydrolyzes to a small extent at pH 6–7 ($K_h = [ZnOH^+][H^+][Zn^{2+}]^{-1} = 10^{-8.8}$),[11,12] and the rate enhancement by the formation of $Zn(OH)^+$ was negligible in the presence of amino acid and at pH <6.5.[13] The plot of $k_{0(Zn,A)}[Zn^{2+}]^{-1}$ versus $[A^-]$ yielded a straight line with an intercept of k_1 and slope of k_2. Thus the last term in eq 2 is not important as expected: both k_3 and $[ZnA_2]$ are low. Typical data for L-tryptophan, L-phenylalanine, and glycine are shown in Figure 1: the rate is higher at high $[A^-]$, i.e. at high pH. The rate constant k_2 was determined from the slope by using β_1 for amino acids: the logarithmic values of β_1 are 4.96, 4.51, 4.44, 4.29, 4.16, and 5.01 for Gly, Ala, Val, Phe, Tyr, and Trp, respectively. The rate constants for the reaction of zinc(II) complex of amino acid with H_2TPPS_4 are summarized in Table I along with the hydrophobicity scale of the amino acid side chain.[9] The bound amino acid enhances the rate of formation of $Zn^{II}(TPPS_4)$ in the order Gly < Ala < Val < Phe < Tyr < Trp. In the presence of Trp the rate is about 50 times as great as that for aquazinc(II). Since the stepwise protonation constants of H_2TPPS_4 to form H_3TPPS_4 and H_4TPPS_4 are $10^{4.99}$ and $10^{4.76}$, respectively,[14] porphyrin is in the free base form at pH 6–7, and dimerization of H_2TPPS_4 ($C_{H_2TPPS_4} = 105 \times 10^{-6}$ mol dm^{-3}) can be negligible.[15,16] Thus

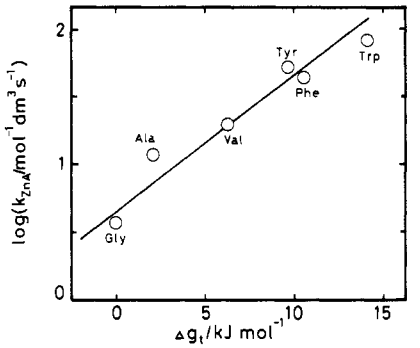

Figure 2. Logarithmic rate constant of reaction of zinc(II) complex of amino acid with H_2TPPS_4 plotted against the hydrophobicity scale of the amino acid side chain (Δg_t/(kJ mol^{-1})).

the reaction sequence of H_2TPPS_4 with zinc(II) in the presence of amino acid may be described as follows:

$$ZnA^+ + H_2TPPS_4 \overset{K}{\rightleftharpoons} \underset{I}{ZnA^+ \cdot H_2TPPS_4} \quad (5)$$

$$I \xrightarrow{k} Zn^{II}(TPPS_4) + A^- + 2H^+ \quad (6)$$

ZnA^+ rapidly associates with free base porphyrin to form a molecular complex (I) in which ZnA^+ is weakly bound to the porphyrin plane. Then the water molecule coordinated to zinc(II) in I dissociates, and zinc(II) is incorporated into the porphyrin core. Thus the overall rate constant (k_{ZnA}) for the reaction of ZnA^+ with H_2TPPS_4 is given by eq 7.

$$k_{ZnA} = Kk \quad (7)$$

One possible role of the bound amino acid is to labilize the water molecule coordinated to zinc(II)[13,17] (i.e. k in eq 7 becomes greater by the coordination of amino acid). The rate constant for the reaction of (glycinato)zinc(II) with H_2TPPS_4 is about 2 times greater than that of the aquazinc(II) (Table I). This is quantitatively interpreted in terms of the increased lability of water molecule by electron donation of nitrogen and oxygen atoms in glycine.[13] A similar labilizing effect is anticipated also for the other amino acids. As shown in Table I, however, the rate constants determined for the other amino acids are larger than that observed for glycine. Another possible role of bound amino acid is the interaction of amino acid with porphyrin. According to eq 7 the larger the formation constant of molecular complex I, the higher the overall formation rate constant of $Zn^{II}(TPPS_4)$. In Figure 2, the rate constant is plotted against the hydrophobicity scale of amino acid side chain. Figure 2 suggests that the rate enhancement by amino acid results from the hydrophobic interaction of zinc(II)–amino acid complex with porphyrin (see eq. 7): L-Trp gives the largest catalytic effect among them.

The catalytic effect of coordinated ligands is not specific to amino acids and has also been observed for pyridine, imidazole, 3,5-disulfonato-1,2-benzenediol (tiron), 8-quinolinol, acetate, and ammonia.[18,19] The copper(II) complex of of tiron or 8-quinolinol reacts with 5,10,15,20-tetrakis(4-*N*-methylpyridyl)porphine (TMPyP) 1000 times faster than with aquacopper(II) ion. The rate enhancement by these aromatic ligands appears to result from the molecular complex formation by hydrophobic interaction between porphyrin plane and aromatic ligand. This effect is greater than the labilizing effect due to the electron donation from bound ligands.[13]

The present paper describes, for the first time, the importance of hydrophobic interaction in the formation of metalloporphyrins.

(10) (a) Martell, A. E.; Smith, R. M. *Critical Stability Constants*; Plenum: New York, 1974; Vol. 1. (b) Perrin, D. D. *Stability Constants of Metal-Ion Complexes, Part B, Organic Ligands*; Pergamon: New York, 1979.
(11) Sillén, L. G.; Martell, A. E. *Stability Constants of Metal-Ion Complexes*; The Chemical Society: London, 1964.
(12) Thompson, A. N.; Krishnamurthy, M. *J. Inorg. Nucl. Chem.* **1979**, *41*, 1251–1255.
(13) Yamada, S.; Ohsumi, K.; Tanaka, M. *Inorg. Chem.* **1978**, *17*, 2790–2794.
(14) Tabata, M.; Tanaka, M. *J. Chem. Soc., Chem. Commun.* **1985**, 42–43.
(15) Fleischer, E. B.; Palmer, J. M.; Srivastava, T. S.; Chatterjii, A. *J. Am. Chem. Soc.* **1971**, *93*, 3162–3167.
(16) Pasternack, R. F.; Francesconi, L.; Raff, D.; Spiro, E. *Inorg. Chem.* **1973**, *12*, 2606–2611.
(17) Margerum, D. W.; Cayley, G. R.; Weatherburn, D. C.; Pagenkopf, G. K. *Coordination Chemistry*; Martell, A. E., Ed.; ACS Monograph 174; American Chemical Society: Washington, DC, 1978; Vol. 2, Chapter 1.
(18) Hambright, P.; Chock, P. B. *J. Am. Chem. Soc.* **1974**, *96*, 3123–3131.
(19) Schneider, W. *Struct. Bonding (Berlin)* **1975**, *23*, 123–166.

Acknowledgment. This investigation was supported by Grants-in Aid for Scientific Research (Nos. 59430010 and 61540450) and a Grant-in-Aid for Special Project Research (No. 60129031) from the Ministry of Education, Science, and Culture (Japan).

Registry No. Zn^{2+}, 23713-49-7; H_2TPPS_4, 35218-75-8; H_2O, 7732-18-5; glycine, 56-40-6; L-α-alanine, 56-41-7; L-valine, 72-18-4; L-phenylalanine, 63-91-2; L-tyrosine, 60-18-4; L-tryptophan, 73-22-3.

Contribution from the Department of Chemistry
and the Rice Quantum Institute,
Rice University, Houston, Texas 77251

Low-Temperature Reactions of Methane with Photoexcited Nickel Atoms

Sou-Chan Chang, Robert H. Hauge, W. E. Billups,*
John L. Margrave,* and Zakya H. Kafafi†

Received March 6, 1987

We have been engaged recently in studies on the isolation and characterization of simple unligated alkylmetal hydrides.[1,2] These species can be prepared readily by photolysis of metal atoms in an inert-gas or neat alkane matrix and characterized by FTIR spectroscopy. In our earlier studies we were surprised to find that we were unable to characterize any species that could be attributed to an insertion product of nickel. We have now reinvestigated the reactions of nickel atoms with methane in both neat matrices and argon matrices using sensitive FTIR characterization,[3] and we find that nickel does indeed insert photolytically into a C–H bond of methane to yield CH_3NiH. Our earlier efforts to detect this species were unsuccessful because of the weak absorptions exhibited by this product.[4]

Experimental Section

A description of the multisurface matrix isolation apparatus has been reported previously.[3] Nickel atoms were obtained by vaporizing nickel metal (Mackay, 99.5%) from an alumina crucible enclosed in a resistively heated tantalum furnace over the range 1350–1500 °C. The temperature was measured with a microoptical pyrometer (Pyrometer Instrument Co.).

In a typical experiment, nickel atoms were codeposited with either methane (Matheson, 99.97%) or methane/argon (Matheson, 99.98%) onto a rhodium-plated copper surface over a period of 10 or 30 min, respectively. The copper block was maintained at 11–14 K by use of a closed-cycle helium refrigerator (Air Products, Displex Model CSW-202). Prior to deposition, the molar ratio of nickel/methane or nickel/methane/argon was measured with a quartz crystal microbalance mounted on the cold block. The molar ratios were 1/10 and 0/1/100 to 1.5/1.8/100, respectively. After deposition, the infrared spectrum of the matrix-isolated species was measured with an IBM IR-98 Fourier-transform infrared spectrometer. The frequencies were measured over the range 4000–300 cm^{-1} to an accuracy of ±0.05 cm^{-1}.

The photolysis studies were usually carried out subsequent to deposition by exposure of the matrices to a focused 100-W medium-pressure short-arc Hg lamp. The typical exposure time was 10 min. A water filter with various Corning long-pass cutoff filters and a band filter, 280–360 nm, was used for the wavelength-dependent photolysis experiment. Carbon-13-enriched methane (Mound Facility, Monsanto, 99 atom % ^{13}C) and deuteriated methane (Icon Service, CD_4 99 atom %) were used in isotopic studies.

† Present address: Naval Research Laboratory, Code 6551, Washington, DC 20375.

(1) Billups, W. E.; Konarski, M. M.; Hauge, R. H.; Margrave, J. L. *J. Am. Chem. Soc.* **1980**, *102*, 7393.
(2) Kafafi, Z. H.; Hauge, R. H.; Fredin, L.; Billups, W. E.; Margrave, J. L. *J. Chem. Soc., Chem. Commun.* **1983**, 1230.
(3) Hauge, R. H.; Fredin, L.; Kafafi, Z. H.; Margrave, J. L. *Appl. Spectrosc.* **1986**, *40*, 588.
(4) The previous studies were carried out with a Beckman IR-9 spectrometer.

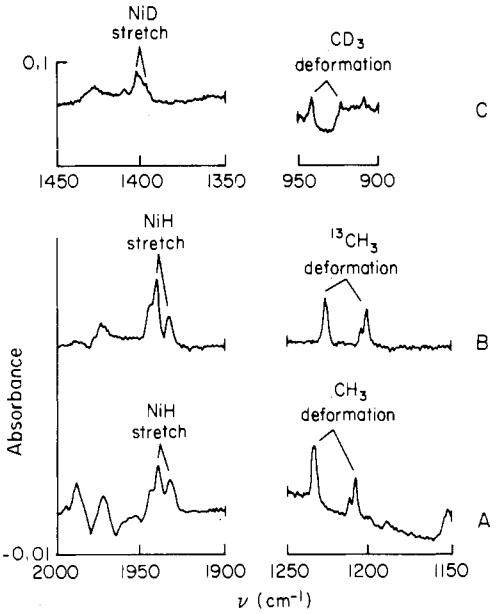

Figure 1. Isotopic study with FTIR specta of CH_3NiH (A), $^{13}CH_3NiH$ (B), and CD_3NiD (C) in methane matrices.

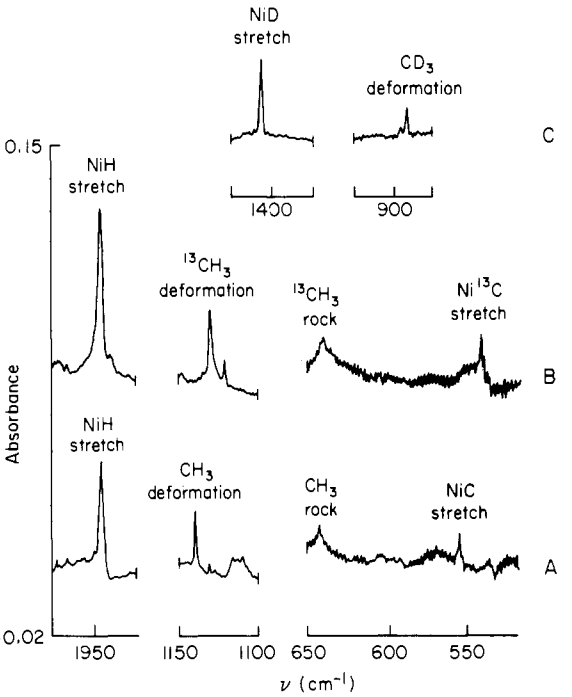

Figure 2. FTIR spectra of CH_3NiH (A), $^{13}CH_3NiH$ (B), and CD_3NiD (C) in argon matrices.

Table I. Measured Infrared Frequencies (cm^{-1}) for CH_3NiH, $^{13}CH_3NiH$, and CD_3NiD in Solid Methane and Solid Argon

	CH_3NiH		$^{13}CH_3NiH$		CD_3NiD	
vib mode	CH_4	Ar	$^{13}CH_4$	Ar	CD_4	Ar
NiC, $Ni^{13}C$ str	551.0	554.9	537.5	542.4		
CH_3, CD_3 rock		642.7		641.0		
CH_3, CD_3 def	1207.7	1120.3	1200.0	1120.4	923.0	891.9
	1233.3	1139.0	1226.4	1129.4	942.0	895.8
NiH, NiD str	1939.2	1945.1	1939.1	1945.3	1402.0	1406.8
CH_3, CD_3 str		2861.0		2855.8		
		2950.5		2940.4	2192.0	2197.5

Results and Discussion

The infrared spectrum of CH_3NiH was observed after UV irradiation of either a nickel/methane or nickel/methane/argon matrix. The stoichiometry of this insertion product and the vibrational mode assignments were confirmed by a nickel atom

0020-1669/88/1327-0205$01.50/0